The mechanical response of porcine adipose tissue

Kerstyn Comley and Norman Fleck[1],

Department of Engineering, Cambridge University, Cambridge, CB1 2PZ, UK

Submitted to the ASME Journal of Biomechanical Engineering

[1] Corresponding author

Abstract

Subcutaneous adipose tissue has been tested in compression and in shear over a wide range of strain rates, from quasi-static to 5700 s^{-1}. In the quasi-static regime the tissue was subjected to fully reversed cyclic loading. A symmetric tensile-compressive response was observed with lock-up at tensile and compressive strains of 25%. Uniaxial compressive tests at high strain rates (1000 s^{-1} – 5700 s^{-1}) were carried out using a split Hopkinson pressure bar with polycarbonate bars. Over the full range of strain rates from quasi-static to high strain rate, the shape of the stress versus strain response is invariant: the stress level scales with the initial modulus E. A one term Ogden energy density function is adequate to describe the data. The harmonic response of the tissue was also measured in compression-compression and in oscillatory shear over a frequency range from zero to 100 Hz and the complex modulus was determined. The real part of the compression modulus, E', is close to the modulus estimated from the quasi-static tests, and the damping factor tan δ is approximately 0.22 over the frequency range employed.

Keywords: Adipose tissue; High strain rate test; Hopkinson bar test; DMA; Rheology; Uniaxial compression

Introduction

Drug delivery devices load subcutaneous adipose tissue over a range of strain rates, depending upon the characteristics of the device. For example, a needle and syringe will strain the tissue at substantially slower rates than a liquid jet injection. Recently, Shergold and Fleck [1] have developed an penetration model for the dermis. In order to apply this model to adipose tissue it is necessary to measure the uniaxial response, preferably over a wide range of strain and strain rates. The purpose of this paper is to measure the uniaxial response of adipose tissue over the practical range from 10^{-4} s^{-1} to 5000 s^{-1}. Both monotonic and cyclic tests are performed, and the large strain response is determined in addition to the viscoelastic characteristics at low strain level.

Microstructure of Adipose Tissue

Adipose tissue, commonly known as fat, is a connective tissue comprising lipid-filled cells called *adipocytes*. The lipid is a triacylglyceride whose molecular weight is in the order of 900 g mol^{-1}. The adipocytes are of diameter 80 μm and are supported by two collagen-based structures: collagen mesh, containing primarily type I and IV collagen, surrounding each cell, and a type I collagen fibre network termed the *interlobular septa*. Additional structures such as blood vessels exist within the tissue. The intervening space is filled with *ground substance*. 60-80% by weight of adipose tissue is lipid, 5-30% is water and the remaining 2-3% is protein [2]. Histology of adipose tissue suggests that it is approximately isotropic in structure and is thereby isotropic in mechanical properties. The large liquid content enforces material incompressibility [3].

The poro-elastic nature of various biological tissues has been observed by many researchers, see for example Barry and Aldis [4] and Mow *et al.* [5]. The degree to which a soft tissue is poro-elastic depends upon the volume fraction of liquid contained within open channels. When this is large, such as for bone, there is a substantial difference in mechanical response in a fully drained test (allowing for liquid flow and egress from the specimen) compared to an undrained test (with no liquid flow). The important feature of poro-elasticity is the fact that the fully drained stiffness is much less than the undrained stiffness. In adipose tissue, the ground substance (which fills the open channels) accounts for only a few percent of the volume fraction and there is negligible free fluid available to endow the tissue with poro-elastic properties. This has been confirmed by preliminary compression tests on porcine adipose tissue. On subjecting the tissue to a uniaxial compressive strain of 50% the volume of liquid expressed was less than 1% of the overall volume. We note in passing that the finite permeability of adipose is an insufficient indicator of poro-elastic behaviour. The measured apparent permeability is very low for adipose tissue and is in the range 1 – 18 x 10^{-13}

$m^4\ s^{-1}\ N^{-1}$ [6, 7].

Review of methods used to measure the constitutive response of soft tissue

The possible asymmetry between tensile and compressive behaviours

The experimental measurement of the constitutive properties of biological tissues tends to focus on either the compressive or tensile properties of the tissue. For example, Miller-Young [8] measured the stress versus strain response of calcaneal fat in unconfined uniaxial compression at strain rates up to 35 s^{-1}. Samani *et al*. [3] used an indentation method to measure the compressive modulus of breast tissue and Zheng and Mak [9] have attempted to determine the properties of soft limb tissue by manual indentation of live subjects. Although there are no data reported in the literature for the tensile properties of adipose tissue, uniaxial tensile data exist for other soft biological tissues. For example, Huang *et al.* [10] performed tensile tests and compression tests on cartilage. When testing soft tissues there is considerable practical difficulty in identifying the zero strain datum; the forces generated at low levels of strain are low and consequently a pre-stretch or pre-tension can be generated within the tissue during insertion into a test machine. This raises the question as to whether the transition point between tension and compression has been accurately identified. Sophisticated methods which attempt to overcome these difficulties have been presented; see for example Mansour [11]. However, these methods do not guarantee that the point of zero strain has been identified. The problem of identifying the zero strain datum is resolved in the current study by performing large amplitude fully reversed strain excursions.

Compressive testing at high strain rates

The split Hopkinson pressure bar (SHPB) is an established technique used to measure the behaviour of many engineering materials at strain rates above about 100 s^{-1}. Van Sligtenhorst [12] and Song *et al.* [13] have compared the SHPB response with the quasi-static response for muscle tissue: they observe an elevation in stress level by a factor of 1000 when $\dot{\varepsilon}$ is increased from 10^{-3} s^{-1} to 10^{3} s^{-1}. However, no data are available on the high strain rate behaviour of adipose tissue. The paucity of data is due in part to the difficulty of applying the split Hopkinson pressure bar method to soft tissues where the measured stresses are low, typically less than 5 MPa. In order to increase the measurement sensitivity modifications are needed to the standard steel bar set-up. Song *et al*. [13] measured the properties of porcine muscle with aluminium pressure bars and Shergold *et al*. [14] used magnesium bars to measure the stress versus strain response of pig skin. In the present study a modified SHPB using polycarbonate (PC) pressure bars is employed in order to measure the

compressive behaviour of adipose tissue at strain rates between 1000 s^{-1} to 5700 s^{-1}. PC is attractive because it has a low modulus of 3 GPa and thereby gives a sensitive response.

Constitutive modelling of soft biological tissues

It is generally recognised that the stress versus strain response of connective tissue has a characteristic J – shape, such that stiffening occurs at strains above about 30%, Purslow [15]. Additionally, the stress level increases with increasing applied strain rate. Since the response is strain rate dependent a strain energy density function does not exist for the material. Despite this deficiency rubber elasticity models provide a useful phenomenological description of the shape of the stress versus strain curve for a given value of strain rate. The Mooney-Rivlin model has frequently been used to model soft tissue [16], however, Shergold *et al.* [14] argue that the Ogden [17] model for an incompressible, isotropic, hyper-elastic solid describes a wide range of strain hardening characteristics for the dermis. The one-term Ogden strain energy density function is given as:

$$\phi = \frac{2\mu}{\alpha^2}(\lambda_1^\alpha + \lambda_2^\alpha + \lambda_3^\alpha - 3) \qquad (1)$$

where ϕ is the strain energy density per undeformed unit volume, λ is the stretch ratio, α is the strain hardening exponent and μ is the shear modulus.

Shergold *et al.* [14] suggest that since the characteristic J-curve is due to alignment of collagen fibres and the degree of fibre alignment is insensitive to strain rate the strain hardening exponent α is strain-rate independent. In contrast the shear modulus is expected to increase with strain rate as it is determined by the rate dependence of the collagen fibres and the surrounding matrix. It will be shown below that the one term Ogden model is adequate to describe the uniaxial compression data of porcine adipose tissue.

Outline of the study

The mechanical response of subcutaneous adipose tissue is examined over a wide range of strain rates, from quasi-static to 5700 s^{-1}. The quasi-static tests entail large amplitude, fully reversed loading in order to probe the non-linear uniaxial response and to determine the degree of asymmetry between the tensile and compressive responses.

Monotonic uniaxial compression tests are also carried out at strain rates ranging from 10^{-4} s^{-1} to

5700 s^{-1}. The uniaxial compressive tests at high strain rates (1000 s^{-1} – 5700 s^{-1}) employ a modified split Hopkinson pressure bar with polycarbonate bars. Additionally, low strain amplitude harmonic tests are performed in compression-compression and in oscillatory shear in order to extract the complex axial modulus and shear modulus as a function of frequency from zero to 100 Hz.

Experimental method

Specimen preparation

It is difficult to acquire fresh human subcutaneous adipose tissue for ethical, immunological and practical reasons. Since porcine adipose tissue has similar morphology, histology and cell kinetics to human adipose tissue [18] it has been chosen as a suitable substitute. Fresh porcine skin tissue was supplied by a local abattoir, Dalehead Foods, Linton. Samples of dermis and subcutaneous fat were removed from the jowl of the pigs to a depth of 20 mm immediately after slaughter. The samples were stored in Phosphate Buffered Saline (PBS) at room temperature prior to testing, which always commenced within 3 hours of slaughter.

Circular cylindrical specimens of adipose tissue were cut to a radius a = 10 mm, with the axis aligned with the normal to the skin using a sharp punch. The specimens were trimmed to a length, l = 3 mm for the high strain rate tests and l = 8 mm for the low strain rate tests. End trimming ensured that the end faces were flat and parallel.

Monotonic compression tests were performed over three regimes:

1. Low strain rate (below 2 s^{-1}), using a screw driven tensile test machine;
2. Intermediate strain rate (20 s^{-1} – 260 s^{-1})), using a servo hydraulic tensile test machine;
3. High strain rate (above 1000 s^{-1}), using a split Hopkinson pressure bar;

Low strain rate compression tests

Cylindrical specimens were compressed between smooth 15 mm thick nylon platens at strain rates of $\dot{\varepsilon} < 0.2$ s^{-1} using a screw-driven tensile test machine. The force generated in the specimens was recorded via a 5 N load cell capable of measuring 20 mN to within 1 %. The initial length of each specimen was taken as the displacement at which a force was first detectable (on the order of 10 mN). Force, displacement and the rate of displacement were converted into nominal engineering

stress, strain and strain rate. Monotonic compression tests were conducted at a strain rate in the range of 2 x 10^{-3} s^{-1} to 0.2 s^{-1}, and were conducted at a strain level of up to 0.4.

Intermediate strain rate compression tests

Specimens were compressed at strain rates from $\dot{\varepsilon}$ = 20 s^{-1} to 260 s^{-1} between smooth nylon platens using a servo-hydraulic test machine and a purpose built load cell [19]. The load cell comprised an aluminium beam, fitted with four strain gauges in a standard Wheatsone bridge arrangement. The stiffness and sensitivity of the beam were 20.46 N mm^{-1} and 141 με N^{-1}, respectively [20]. The displacement of the machine platens was measured using a Linear Resistance Displacement Transducer (LRDT) mounted as an integral part of the test machine. Care was taken to subtract off the machine (and load cell) compliance from the measured displacement response. The outputs from the beam transducer and LRDT was recorded on an oscilloscope and converted into nominal engineering stress, strain and strain rate.

High strain rate compression tests

High strain rate compression tests, above 1000 s^{-1}, were conducted using a Split Hopkinson Pressure Bar (SHPB), see for example Follansbee [21]. The theory of the SHPB is summarised as follows. The input and output bars each has a cross-sectional area A_b and modulus E_b. A specimen of length l and cross-sectional area A_h is placed between them (see Fig. 1a). A striker bar is fired down a gun barrel to impact the input bar. The velocity of the striker bar is measured by light sensors within the gun barrel. On impact, a compression wave (incident wave, i) propagates along the input bar at the speed of sound in the bar. After the incident wave has reached the distal end of the input bar, the distal end begins to compress the specimen. A compression wave is transmitted through the specimen into the output bar (transmitted wave, t), while the remainder of the incident wave is reflected back into the input bar as a tensile wave (reflected wave, r). Strain gauges mounted on the bars measure the axial strain associated with these longitudinal waves.

A full derivation of equations used to calculate the average stress $\sigma_s(t)$, strain $\varepsilon_s(t)$ and strain rate $\dot{\varepsilon}_s(t)$ within the specimen is given by Wang *et al.* [22]. The stress and strain are responses are given by

$$\sigma_s(t) = \frac{E_b A_b}{A_h} \varepsilon_t(t) \tag{2}$$

and

$$\varepsilon_s(t) = \frac{2c_b}{l}\int_0^t \varepsilon_r(t)dt \qquad (3)$$

where c_b is the longitudinal wave speed in the pressure bar. It is clear from Eq. (2) that the measured strain level in the output bar, ε_t is dependent upon the ratio of the stress in the specimen, $\sigma_s(t)$ to the modulus of the bar, E_b. If the specimen is very soft (as in the case of adipose tissue) the use of metallic pressure bars results in a low level of transmitted strain and this may be difficult to distinguish from the inherent noise of the test equipment. Also, the input force cannot be precisely measured, which leads to difficulty identifying the force equilibrium point [23].

The strain sensitivity can be increased by using polymeric bars, which have substantially lower elastic moduli than metals. The improvement in sensitivity of the system enables lower stress levels to be measured, and permits a straightforward examination of the force equilibrium in the specimen, in turn giving confidence that the specimen is subjected to uniform deformation with negligible influence of internal wave reflections. In addition, polymers exhibit lower wave speeds than metals and so the specimen can be subjected to a longer test time and thence to larger strains prior to the influence of waves reflected from the ends of the bars [24]. The pressure bars used in this investigation were of diameter 12 mm and were made from cast Polycarbonate. The input and output bars were of length L_b = 1.1 m and the striker bar was of length 0.25 m. Electrical resistance strain gauges were bonded at mid-length of the input and output bars, as shown in Fig. 1a. The gauges were placed in diametrically opposed pairs in order to check for bending.

Use of polycarbonate bars in a Split Hopkinson Pressure Bar

Polymeric bars typically exhibit viscoelastic rather than elastic behaviour which leads to a number of challenges for the analysis of the SHPB data. However, it is clear from the values published by Wang *et al.* [22] that the magnitude of dispersion and attenuation effects are minor for PC bars. Deshpande and Fleck [25] argue that the viscoelastic elastic effects are negligible in PC bars such that they can be assumed to behave in an elastic manner. A series of checks have been conducted to confirm this. From the results it is evident that at low levels of strain (~7 mε) within the PC bars the stress waves propagate along the bars with minimal dispersion. As a final validation exercise the stress versus strain response of Divinycell HD250 PVC foam was measured using PC bars and with magnesium pressure bars.

A separate SHPB set-up was used to run the validation checks, which comprised an input bar of length 2.2 m and a striker of length 0.25 m (Fig. 1b). Both bars were of diameter 12 mm. Pairs of

resistance strain gauges were axially bonded at either end of the input bar, diametrically opposite to each other in order to check for bending. In order to avoid end effects the strain gauges were mounted 0.25 m from the end of the bars, which satisfies the criterion of more than 10 bar diameters from the end of the bar [21]. The sensing circuitry and the calibration method were validated by performing a dummy test using steel bars with no specimen present; the measured strain histories were found to be in good agreement with the predicted values (as given by elastic analysis). The following checks were made to confirm that at low strain levels the PC bars behaved in an elastic manner.

Attenuation of waves in bar

The harmonic solution for the propagation of a longitudinal wave at displacement u in a viscoelastic solid takes the form [26]

$$u = Ae^{\pm\beta x}e^{i\,(\omega t \pm kx)} \tag{4}$$

where β is the wave attenuation, ω is the angular frequency and k is the wave number. A minus sign corresponds to waves propagating in the positive x-direction. The level of attenuation is quantified by the parameter

$$\beta = \frac{\ln(\varepsilon_1/\varepsilon_2)}{x_g} \tag{5}$$

where ε_1 and ε_2 are the maximum strains measured by the first and second strain gauges, respectively, as shown in Fig. 1b; x_g = 1.3 m is the distance between the strain gauges. A typical strain response at the two locations of the input bar is given in Fig. 2a. The average measured level of attenuation was $\beta = 0.012$ m^{-1}. This level of attenuation is considered to be insignificant for selected values of striker velocities, v, in the range 4 – 13 m s^{-1}.

Measurement of dispersion via the evolution of pulse shape along bar

The strain gauge measurements revealed that the strain pulse progressing along the input PC bar is a well-defined square wave, see the typical example shown in Fig. 2a. The viscoelastic tail, as observed by Zhao [23] for PMMA, is not significant for the case of PC, and the waveshape does not change significantly as the wave propagates along the bar. These are typical characteristics of an elastic bar.

Consistency check on the Young's modulus of PC

The Young's modulus of the bar can be predicted from the raw data in two ways [26]:

$$E = c_b^2 \rho \tag{6}$$

or

$$E = \frac{\rho v^2}{4\varepsilon_{\max}^2} \tag{7}$$

where ρ is the density of the bar, c_b is the elastic wave speed and v is the velocity of the striker bar and ε_{max} is the peak height of the square strain pulse.

The predictions according to the two methods are given in Table 1. They agree to within 5% for the PC bar, in support of the assertion that the PC bars can be treated as elastic.

c_b (m s^{-1}) ± 1 s.d.	β (m^{-1})	*E* (GPa] calculated from (3.3)	*E* (GPa) calculated from (3.4)
1495 ±10.7	0.012 ±16 x10^{-4}	4.03 ±0.057	3.84 ±0.002

Table 1: Strain wave analysis in polycarbonate bars. s.d. denotes standard deviation.

Effect of strain amplitude upon the wave speed in the PC bar

The speed of the elastic wave in a bar was measured explicitly from the time taken for the leading edge of the strain wave to travel between the strain gauges. Speed measurements were conducted for a range of peak strains in order to assess whether the wave speed is independent of strain level. The wave speed was not found to depend on strain for peak strains between 1500 με and 4000 με and had a mean value of 1495 m s^{-1}.

As a final validation a high strain rate compression test was performed using the test setup shown in Fig. 1a at a strain rate of 1500 s^{-1} on Divinycell PVC HD250 foam using polycarbonate bars and a repeat test was performed using AZM magnesium alloy pressure bars (supplied by Newmet Kock, Waltham Abbey). The observed responses overlap to within material scatter, see Fig. 2b. The results are also in agreement with those obtained previously by Tagarielli *et al.* [27] using magnesium alloy pressure bars.

Dynamic mechanical analysis (DMA) and oscillatory shear tests

Cyclic tensile and compression tests

Using the set-up described in section 2.2.1 additional, fully reversed loading experiments were conducted to compare the tensile and compressive behaviours of the tissue. The upper and lower faces of the specimens were bonded to the platens using a cyanoacrylate adhesive (Loctite® Super Glue^{TM} Control Liquid). A periodic triangular displacement profile was used to cycle the specimens between a tensile and compressive strain at a strain rate of approximately 0.07 s^{-1}. Prior to testing a pilot study was conducted to examine whether the imposed mechanical constraint associated with bonding the tissue to the displacement platens resulted in an increase in the measured stress during compression. No significant difference was observed between bonded and unbonded specimens.

Measurement of complex compression modulus, 20 Hz – 100 Hz

An experimental rig was used to measure the oscillatory uniaxial compressive properties of adipose tissue. Circular cylindrical specimens of diameter d = 11mm and length l =11 mm were compressed between two nylon platens. The lower platen was attached to a V201 moving coil shaker (Link Dynamic Systems, Herts, UK), and this in turn was driven by a 'pink noise' generator with a frequency cut off of 500 Hz. The amplitude of displacement used in the tests was in the range 4 μm to 50 μm, giving a strain amplitude of 0.1 – 1 %. The upper platen was attached to a piezoelectric force sensor with a sensitivity of 115 pC N^{-1} and a natural frequency of >10 kHz (9205, Kistler, Winterhur, Switzerland), and the transducer was rigidly attached to the test frame. Piezoelectric accelerometers (Endevco, San Juan Capistrano, USA) were also fastened to the faces of each platen. At 100 Hz the accelerometers had a sensitivity of 0.1388 pC s^2 m^{-1}. Following the suggestion of Yamashita [28] a compressive pre-strain of approximately 15 % was applied to ensure stable measurements of the complex modulus. Prior to testing checks were made to confirm that the viscoelastic stress versus strain response was linear for strain amplitudes of up to 1 %.

The dynamic response and measurement accuracy of the apparatus was verified by performing a dummy test on a compliant aluminium-ring specimen; this circular ring was fitted with a pair of resistance strain gauges and thereby performed as an independent load cell. The stiffness of the load cell was measured as 1.5 N mm^{-1} from an independent test in a screw-driven tensile test machine. The natural frequency of the ring was calculated to be above 4 kHz. The measured stiffness was constant and equal to the quasi-static value to within ±5 % over a frequency range of 20 Hz – 100 Hz.

The complex compression modulus E^* was determined from the harmonic compression tests on adipose tissue as follows. The measured force, $F(t)$, and displacement, u(t), time series data were converted into the frequency domain, $F(\omega)$ and $u(\omega)$, using the fast Fourier transform. The complex modulus E^* of the adipose tissue specimen was calculated via:

$$E^* = E' + iE'' = \frac{F(\omega)l}{u(\omega)A} \tag{8}$$

where A is the cross-sectional area of the specimen; the real part of E^* is the compressive storage modulus E' while the imaginary part is the compressive loss modulus E''.

Measurement of complex shear modulus, 0 – 16 Hz

The oscillatory shear response of adipose tissue has also been measured at a frequency from zero to 16 Hz. A stress controlled rotational rheometer (Bohlin, Malvern Instruments, Malvern, UK) was employed, with 25 mm diameter serrated parallel plates fitted with a temperature controlled oven. First, the large strain response of the tissue was measured by oscillatory shear tests (strain sweeps) at a constant frequency of 1.6 Hz over a range of shear strain amplitudes from 0.03 % - 350 %. Second, oscillatory shear tests (frequency sweeps) were carried out over a frequency range of 0 – 16 Hz, at a constant strain of 1%. Both types of test was conducted at 25 °C and 37 °C, and the values of shear modulus G' and shear loss modulus G'' were recorded.

Results

Monotonic tests

Results from uniaxial compression tests at low strain rates (2×10^{-3} s^{-1} – 2 s^{-1}) and at intermediate strain rates (20 s^{-1} – 260 s^{-1}) are given in Fig. 3. All tests were conducted at room temperature in ambient air at 25 °C and 50% relative humidity. Additional low strain rate tests were carried out to more closely mimic *in-vivo* conditions: the tissue was fully saturated in saline at 37ºC. These results are included in Fig. 3a: there is no significant difference in response between the simulated *in-vivo* conditions and the air tests at room temperature.

Split Hopkinson pressure bar tests were performed at a strain rate of 1000 s^{-1} to 5700 s^{-1}. A representative oscilloscope trace of the strain history in the pressure bars is shown in Fig. 4 for a

strain rate of 1840 s^{-1}. The strain history in the input bar is the characteristic square pulse expected for a linear, elastic impact event between striker and input bar. It is clear from the large value of strain (on the order of 1 mε) detected in the output bar that PC is a suitable choice in terms of sensitivity. Results for the uniaxial compression of adipose tissue, using a split Hopkinson pressure bar at strain rates of 1000 s^{-1} to 5700 s^{-1} are reported in Fig. 3c.

Dynamic mechanical analysis (DMA) and oscillatory shear results at high strain rates

The measured quasi-static stress versus strain response of adipose tissue under fully reversed loading is shown in Fig. 5a. The results are presented as the averaged stress over four cycles for a representative specimen. The levels of force measured in the central linear portion of the curve are on the order of 50 mN, making it difficult to identify the point of zero strain. Therefore, the zero strain datum was taken as mid-way between the points of strain at which the stress equals ± 1 kPa.

The data takes the form of a hysteresis loop with the central portion of the curve spanning a strain range of 50 %. This portion is approximately linear with a tangent modulus of 1 kPa. At strains greater than approximately ± 25 % strain the tissue 'locks up'. The shapes of the tensile and compressive portions are compared in Fig. 5b and are almost symmetric. This contrasts with the pronounced asymmetry of other biological tissues such as cartilage and bone [10] [29].

Cyclic compression tests were performed from zero to peak load at 20 Hz – 100 Hz at a strain amplitude of up to 1%. A linear visco-elastic response was observed (not shown), with a compressive modulus E' equal to 1.8 kPa ± 0.8 kPa, and a loss modulus E'' equal to 0.4 kPa ± 0.2 kP, both independent of frequency. Consequently, the damping factor is $\tan\delta$ =0.22.

The fully reversed, shear viscoelastic response was measured at 0.01 – 16 Hz and at a temperature of 25 ºC, using a shear strain amplitude of 1 %. Preliminary tests at 1 Hz confirmed that the stress response is linear up to a strain amplitude of 5%. It was found that the complex shear modulus is independent of frequency and is given by G' = 530 Pa ± 250 Pa and G'' = 110 Pa ± 60 Pa. Additional tests conducted at 37 ºC suggest that the tissue becomes softer and less viscous with increasing temperature: G' and G'' reduce to 187 Pa and 57 Pa, respectively. The damping factor is $\tan\delta$ =0.30, which is slightly above the tensile value of 0.22, see above. However, the variation between samples is of similar magnitude to the drop in values with increasing temperature. The

measurements of the shear and viscous modulus (G', G'') are consistent with those measured by Patel [30], who gives of G' =1.1 kPa and G'' = 0.6 kPa during tests on adipose at 37 ºC and Geerlings [31], who recorded values of G' = 7.5 kPa and G'' = 2.5 kPa during rheological tests on adipose at 20 ºC.

Discussion

Assessment of the high strain rate results

Application of the SHPB for soft solids requires an assessment of the axial equilibrium and radial inertia within the specimen. Davis and Hunter [32] have demonstrated that a specimen achieves axial equilibrium once an elastic stress wave has passed along its length approximately three times. The time taken for the stress wave to traverse the specimen length is given by l/c_s, where l is the length of the specimen and the elastic wave speed in the specimen c_s depends upon the bulk modulus k according to $c_s = \sqrt{k/\rho}$ [26]. The density ρ of adipose tissue is 920 kgm^{-3}. Saraf *et al.* [33] have estimated the bulk modulus of biological tissue to be approximately 0.5 GPa, giving a wave speed of approximately 700 ms^{-1}. For a specimen length of 3 mm the time taken to reach axial equilibrium is just over 13 μs. The finite rise time of the data acquisition system was on the order of 50 μs, and corresponds to an axial strain of about 5% (see Fig. 6a). It is concluded that axial equilibrium is achieved at an early stage of the test.

Consideration of radial equilibrium for a compression wave propagating along a bar of finite diameter reveals dispersion effects, see Pochhammer [34] and Chree [35]. A representative input pulse has been assessed for dispersion using Bancroft's [36] solution to the Pochhammer Chree equations. The level of dispersion was found to be negligible.

A contribution to the axial stress at high strain rates arises from the finite radial inertia of the specimen. In a high strain rate test on muscle Song *et al.* [13] reported that at low strains (< 20 % strain) the magnitude of radial inertia is comparable to the measured stress response. A representative measure of the stress versus strain response of adipose tissue at $\dot{\varepsilon} = 3500$ s^{-1} is given in Fig. 6b. We note that there is an initial transient in the axial stress with a peak value of 0.5 MPa over an initial compression phase of 10 % strain. We argue that this transient is due to the radial acceleration of material elements (as the velocity of the front face rises from zero to the order of 10 m/s).

Samanta [37] has extended the work of Davies and Hunter [32] and Kolsky [38] to estimate the level of inertial stresses in a material under compression at high speed. The inertial contribution, σ_I to the axial stress comprises a term σ_{vel} associated with the velocity u of the front face of the specimen, and a term σ_{accel} associated with the acceleration du/dt of the front face of the specimen, where

$$\sigma_{vel} = \frac{3}{16}\rho\frac{a^2}{l^2}u^2$$
$$\sigma_{accel} = \rho\left(\frac{a^2}{8l} + \frac{l}{3}\right)\frac{du}{dt} \qquad (9)$$

Here, d is the radius of the specimen, and l is the height of the specimen.

Now substitute some typical values. Consider a test performed at $\dot{\varepsilon}$ = 3500 s^{-1}. The velocity of the front, impacted face of the specimen rises to a value of u = 8 m s^{-1} over the first 30 μs (see Fig. 4). Numerical differentiation of the velocity profile suggests that acceleration of the material reaches a peak value of du/dt = 3 x 10^5 m s^{-2}. The contributions of σ_{vel} and σ_{accel} to the inertial stress σ_I, of a specimen tested at $\dot{\varepsilon}$ = 3500 s^{-1} are shown in Fig. 6b and are compared to the measured stress versus strain curve. The peak value of σ_I is approximately 0.1 MPa at 2 % strain and falls to zero by 5 % strain. This analysis indicates that at strain levels less than 5 % the stress measurement is dominated by inertial stress. All subsequent interpretation of the data at high strain rates is, therefore, restricted to measurements made at 5 % strain and above. The Young's modulus is taken as the secant value at a strain level of 10%, in order to disregard the inertial contribution.

The behaviour of adipose tissue in comparison with other connective tissues

A comparison can be made of the monotonic data over the full range of strain rate (Fig. 3). The shape of the stress versus strain curves is invariant with regard to strain rate while the stress level is sensitive to strain rate. The uniaxial compressive stress σ has been normalised by the measured Young's modulus E at any given $\dot{\varepsilon}$ and is plotted against strain in Fig. 7a; the data collapse onto a single master curve. This geometric similarity has been noted previously by Shergold and Fleck [14] for porcine dermis and leads to a considerable simplification of the constitutive description. The σ / E versus ε curve for the dermis (averaged over strain rates from 10^{-3} s^{-1} to 10^3 s^{-1}) is included in Fig. 7a; the normalised response is similar to that for adipose tissue, with a larger lock-up strain of order 0.4 compared to 0.25 for adipose tissue.

The dependence of E upon $\dot{\varepsilon}$ is shown in Fig. 7b. For strain rates in the range 2 x 10^{-3} s^{-2} to 10 s^{-1} the Young's modulus E equals approximately 1 kPa and is insensitive to strain rate. This measured value is in good agreement with previous measurements for adipose tissue, as follows: Samani [3] used indentation to measure an elastic modulus of 1.9 kPa for breast tissue and Nightingale [39] measured a value of 5 kPa for human abdominal subcutaneous tissue using acoustic radiation force impulse imaging (ARFT). For strain rates in the range of 10 s^{-1} to 5700 s^{-1} the Young's modulus is sensitive to strain rate and increases by three orders of magnitude from E = 2 kPa at $\dot{\varepsilon}$ = 10 s^{-1} to approximately E = 4 MPa at $\dot{\varepsilon}$ = 2000 s^{-1}. A similar sensitivity has been observed for muscle by Van Sligtenhorst *et al.* [12] and Song *et al.* [13]. The dependence of E upon $\dot{\varepsilon}$ for porcine dermis is taken from Shergold *et al.* [14] and is included in Fig. 7b (and Table 2). We conclude that the dermis is stiffer by more than two orders of magnitude at low strain rates but has a comparable response at high strain rates.

A constitutive description using the Ogden model

A modified one-term Ogden [17] strain energy density function ϕ is used to describe the constitutive behaviour of adipose tissue. The principal values of nominal stress σ_i (i = 1, 2, 3) are related to the principle stretches λ_i by

$$\sigma_i = \frac{d\phi}{d\lambda_i} - p \tag{10}$$

where p is the hydrostatic pressure.

During uniaxial compression the specimen is assumed to be in a state of uniaxial stress with the z-axis of a Cartesian co-ordinate system aligned with the direction of the applied load. Therefore,

$$\sigma_x = \sigma_y = 0 \tag{11}$$

For an incompressible solid in which the volume is conserved the principle stretch ratios are related by

$$\lambda_x = \lambda_y = \frac{1}{\sqrt{\lambda_z}} \tag{12}$$

And λ_i is related to strain ε_i, by

$$\varepsilon_i = -\ln \lambda_i \tag{13}$$

Therefore, Eq. (1) can be re-written as

$$\sigma = \frac{2\mu}{\alpha}[e^{-\varepsilon(\alpha-1)} - e^{\varepsilon(1+\frac{\alpha}{2})}] \qquad (14)$$

where α is a strain hardening exponent and μ is the shear modulus under infinitesimal straining.

The Ogden model Eq. (14) has been fitted to all the uniaxial compression data across the full range of strain rates tested. The shear modulus μ was taken as $E/3$ for each stress versus strain curve. A value of $\alpha = 20$ gives the best fit to the data. The average value of μ within each strain rate regime of testing is given in Table 2. Previous results for μ for the dermis, taken from Shergold et al. [14], are also included. For the dermis the exponent has a value of $\alpha = 12$ over the full range of strain rates explored.

	Adipose	**Dermis**
$\dot{\varepsilon}$ **(s^{-1})**	μ **(kPa)**	μ **(kPa)**
0 – 10	0.4	400
20 – 260	1.7	2200
1000 - 5700	1120	7500

Table 2: Best fit values (for μ) for a one term Ogden strain energy density function of adipose and dermal tissue evaluated at different strain rates, $\dot{\varepsilon}$ [s^{-1}]. Values for the dermis are given by Shergold *et al*. [14].

Relevance of dynamic mechanical analysis (DMA) and oscillatory shear tests to the uniaxial tests

The measured values of compression and shear modulus are summarised in Table 3 for uniaxial tests at strain rates below 2 s^{-1} and for the cyclic uniaxial and shear tests. Adequate agreement is noted between the Young's modulus E = 1 kPa as measured by uniaxial compression tests at $\dot{\varepsilon}$ below 10 s^{-1} and E' = 1.8 kPa from the viscoelastic measurements. It is also noted that $G' \approx E'/3$ as expected for an isotropic, incompressible solid. The degree of damping is small over the range considered. The harmonic response of adipose tissue at frequencies up to 100 Hz suggests that the tissue can be treated as a linear viscoelastic solid at small strain amplitudes.

The mechanical properties of adipose tissue

Young's modulus E	1 kPa ± 0.1 kPa
Compression modulus E'	1.8 kPa ± 0.8 kPa
Shear modulus G'	0.53 kPa ± 0.25 kPa
Loss modulus E''	0.4 kPa ± 0.2 kPa
Loss modulus G''	0.11 kPa ± 0.06 kPa

Table 3: Measured values of compression and shear modulus from uniaxial tests at strain rates below 2^{-1} and from cyclic uniaxial and shear tests.

Concluding remarks

The constitutive properties of adipose tissue have been measured over a wide range of strain rate from 2 x 10^{-3} s^{-1} to 5700 s^{-1}. The shape of the compressive stress versus strain curve is similar across all strain rates, differing only by a scale factor which is conveniently given by the Young's modulus. This allows for a major simplification in description of the constitutive response. A one term Ogden strain energy density model can be used to adequately describe the data over the strain rates tested. This model comprises two parameters, the strain hardening exponent α (independent of strain rate) and the shear modulus μ (which scales with strain rate). It has also been shown that at small strain amplitudes, up to frequencies of 100 Hz the tissue behaves as a linear viscoelastic solid.

Acknowledgements

The authors are grateful for financial support by the EPSRC and by Novo Nordisk A/S, Denmark.

References

[1] Shergold, O. A. and Fleck, N. A., 2004 *Mechanisms of deep penetration of soft solids, with application to the injection and wounding of skin* Proc. R. Soc. London ser A, **460**, pp. 3037-3058

[2] Greenwood, M. R. C. and Johnson, P. R., 1983 *The adipose tissue*, In: Weiss, L.(eds) Histology, cell and tissue biology, Edition 5, Macmillan

[3] Samani, A., *et al*., 2003, *Measuring the elastic modulus of ex vivo small tissue samples*, Phys. Med. Biol., **48**, pp. 2183-2198

[4] Barry, S. I. and Aldis, G. K., 1990, *Comparison of models for flow induced deformation of soft biological tissue*, J. Biomech., **23**, pp. 647-654

[5] Mow, V. C., *et al*., 1980 *Biphasic creep and stress relaxation of articular cartilage in compression: theory and experiments*, J. Biomech. Eng., Trans. ASME, **102**, pp. 73-84

[6] Guyton, A. C., *et al*. 1966, *Interstitial fluid pressure. 3. Its effect on resistance to tissue fluid mobility*, Circ. Res., **19**, pp. 412-9

[7] Reddy, N. P. and Cochran, G. V. 1981, *Interstitial fluid flow as a factor in decubitus ulcer formation*, J. Biomech., **14**, pp. 879-81

[8] Miller-Young, J. E., *et al*. 2002, *Material properties of the human calcaneal fat pad in compression: Experiment and theory*, J. Biomech., **35**, pp. 1523-1531

[9] Zheng, Y. P. and Mak, A. F. T. 1999, *Extraction of quasi-linear viscoelastic parameters for lower limb soft tissues from manual indentation experiment*, J. Biomech. Eng., **121**

[10] Huang, C.-Y., *et al*. 2005, *Anisotropy, inhomogeneity, and tension-compression nonlinearity of human glenohumeral cartilage in finite deformation*, J. Biomech., **38**, pp. 799-809

[11] Mansour, J. M., *et al*. 1993, *A method for obtaining repeatable measurements of the tensile properties of skin at low strain*, J. Biomech., **26**, pp. 211-6

[12] Van Sligtenhorst, C., *et al*. 2006, *High strain rate compressive properties of bovine muscle tissue determined using a split Hopkinson bar apparatus*, J. Biomech.;39;1852-1858

[13] Song, B., *et al*. 2007, *Dynamic and quasi-static compressive response of porcine muscle,* J. Biomech., **40**, pp. 2999-3005

[14] Shergold, O., *et al*. 2006, T*he uniaxial stress versus strain response of pig skin and silicone rubber at low and high strain rates*, Int J. Impact Eng., **32**,9, pp. 1384-1402

[15] Purslow, P. 1991 *Notch-Sensitivity of Nonlinear Materials* J Mat Sci, **26** pp. 4468-4476

[16] Miller, K. and Chinzei, K. 1997, *Constitutive modelling of brain tissue: Experiment and theory*, J. Biomech., **30**, pp. 1115-1121

[17] Ogden, R. W. 1972, *Large Deformation Isotropic Elasticity - Correlation of Theory and Experiment for Incompressible Rubberlike Solids*, Proc. R. Soc London Ser A, **326**, pp. 565

[18] Douglas, W. R. 1972, *Pigs and Men and Research - Review of Applications and Analogies of Pig*, Sus Scrofa, in Human Medical-Research, Space Life Sciences, **3**, pp. 226

[19] Doebelin, E. O. 1966, *Measurement systems: Application and design*, McGraw-Hill

[20] Fleck, N. A. 1983, *Some aspects of clip gauge design*, Strain, **19**, pp. 17-22

[21] Follansbee, P. S. 1985, *The Hopkinson bar*, In: H. Kuhn and D. Medlin, E.(eds) ASM Handbook: Volume 8 mechancial testing and evaluation ASM International

[22] Wang, L. *et al.* 1992, *Generalization of split Hopkinson bar technique to use viscolelastic bars*, Int. J. Impact Eng., **15**, pp. 669-686

[23] Zhao, H. *et al*. 1997, *On the use of viscoelastic split Hopkinson pressure bar*, Int J. Impact Eng., **19**, pp. 319-330

[24] Sawas, O. *et al*. 1998, *Dynamic characterisation of compliant materials using an all-polymeric split Hopkinson bar*, Exp Mech, pp. 204-210

[25] Deshpande, V. S. and Fleck, N. 2000, *High strain rate compressive behaviour of aluminium alloy foams*, Int. J. Impact Eng., **24**, pp. 277-298

[26] Kolsky 1953 *Stress waves in solids*, Oxford

[27] Tagarielli, V. L. *et al*. 2008, *The high strain rate response of PVC foams and end-grain balsa wood*, Composites Part B: Eng. Marine Composites Sandwich Struc., **39**, pp. 83-91

[28] Yamashita, J. *et al*. 2001, *The use of dynamic mechanical analysis to assess the viscoelastic properties of human cortical bone*, J Biomed Mater Res, **58**, pp. 47-53

[29] Knothe Tate, M. L., R. Steck, et al. (2009), *Bone as an inspiration for a novel class of mechanoactive materials*. Biomat **30**(2): 133-140

[30] Patel, P. N. *et al*. 2005, *Rheological and recovery properties of poly(ethylene glycol) diacrylate hydrogels and human adipose tissue*, J. Biomed. Mat. Res. Part A, **73A**, pp. 313-31

[31] Geerligs, M., G. W. M. Peters, et al. (2008), *Linear viscoelastic behavior of subcutaneous adipose tissue*. Biorheol **45**(6): 677-688

[32] Davies, E. D. H. and Hunter, S. C. 1963, *The dynamic compression testing of solids by the method of the split Hopkinson pressure bar*, J. Mech. Phys. Solids, **11**, pp. 155-179

[33] Saraf, H. *et al*., 2007, *Mechanical properties of soft human tissues under dynamic loading*, J. Biomech., **40**, pp. 1960-1967

[34] Pochhammer, L. 1876, J. Reine Angew. Math., **81**, pp. 324

[35] Chree, C. 1889, Trans. Camb. Phil. Soc., **14**, pp. 250

[36] Bancroft, D. 1941, Phys. Rev., **59**, pp. 588

[37] Samanta, S. K. 1971, *Dynamic deformation of aluminium and copper at elevated temperatures*, J. Mech. Phys. Solids, *19*, pp. 117-122

[38] Kolsky, H. 1949, *An investigation of the mechanical properties of materials at very high rates of loading*, Proc. R. Soc. London, Ser. B, **62**, pp. 676-700

[39] Nightingale, K. *et al*. 2003, *Shear-wave generation using acoustic radiation force: In vivo and ex vivo results*, Ultrasound Med. Biol., **29**, pp. 1715-1723

The mechanical response of porcine adipose tissue

Kerstyn Comley and Norman Fleck
FIGURES
Submitted to the ASME Journal of Biomechanical Engineering

Table 1: Strain wave analysis in polycarbonate bars.

Table 2: Best fit values (for μ) for a one term Ogden strain energy density function of adipose and dermal tissue evaluated at different strain rates, $\dot{\varepsilon}$ (s^{-1}). Values for the dermis are given by Shergold et al. [14].

Table 3: Measured values of compression and shear modulus for uniaxial tests at strain rates below 2 s^{-1} and cyclic uniaxial and shear tests.

Figure 1: (a) Experimental setup of the split Hopkinson pressure bar (SHPB). (b) Modified SHPB used to validate elastic behaviour of Polycarbonate (PC) pressure bars. Dimensions are in mm.

Figure 2: (a) Typical strain response of the long polycarbonate bar measured at two locations along the bar. The impact velocity of the striker is approximately v = 10 m s^{-1}. The distance between the first strain gauge and the second strain gauge is 1.3 m. (b) Compression of Divinycell PVC HD250 foam. Results obtained with polycarbonate pressure bars are compared to results collected using magnesium pressure bars. The tests were conducted at a strain rate of 1500 s^{-1}.

Figure 3: Uniaxial compression of adipose tissue at strain rates (a) $\dot{\varepsilon}$ = 0.002 s^{-1} – 0.25 s^{-1}. (b) $\dot{\varepsilon}$ = 20 s^{-1} – 260 s^{-1}. (c) $\dot{\varepsilon}$ = 1000 s^{-1} - 5700 s^{-1}. Data in graph (a) represented by a solid line was measured at 25 ºC, representative data at 37 ºC is shown by a dashed line.

Figure 4: Oscilloscope trace of the compression of adipose tissue using a split Hopkinson pressure bar at a strain-rate of 1840 s^{-1}.

Figure 5: (a) Quasi-static uniaxial compression and tension of adipose tissue averaged over 4 cycles. Arrows show the direction of displacement. The data has been shifted relative to the strain axis so that strain is equi-distant between ± 1 kPa stress. (b) Quasi-static uniaxial tension versus compression of adipose tissue.

Figure 6: (a) Comparison of input ($\sigma_i + \sigma_r$) and output (σ_t) stress measured by the SHPB to assess the time to reach axial equilibrium. Measurements were taken at a nominal strain rate of 2000 s^{-1}. (b) Comparison of the measured stress with the inertial stresses σ_{vel} and σ_{accel}, described by Eq. (9). The net response is the measured stress less the inertial stresses. The test was conducted at 3500 s^{-1}.

Figure 7: (a) Stress versus strain curves of adipose tissue, normalised by modulus E. The average dermal response measured by Shergold et al. [14] is shown for comparison. (b) Modulus, E (Pa) of

adipose tissue under uniaxial compression versus strain rate (s^{-1}). Data shown by triangular markers were measured using a screw-driven tensile test machine, circular markers by a hydraulic test machine and the crosses represent data collected using the SHPB. Diagonal crosses represent the modulus of dermis recorded by Shergold et al. [14].

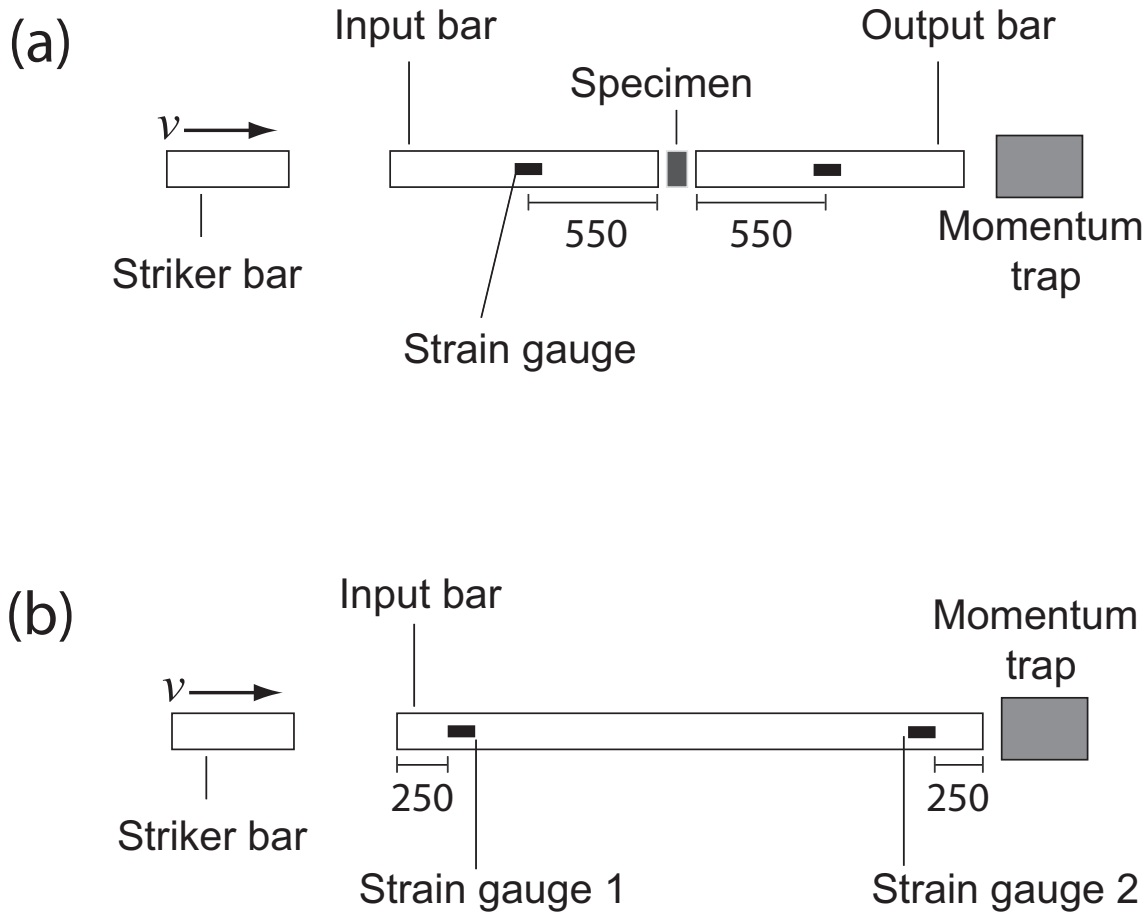

Figure 1: (a) Experimental setup of the split Hopkinson pressure bar (SHPB). (b) Modified SHPB used to validate elastic behaviour of Polycarbonate (PC) pressure bars. Dimensions are in mm.

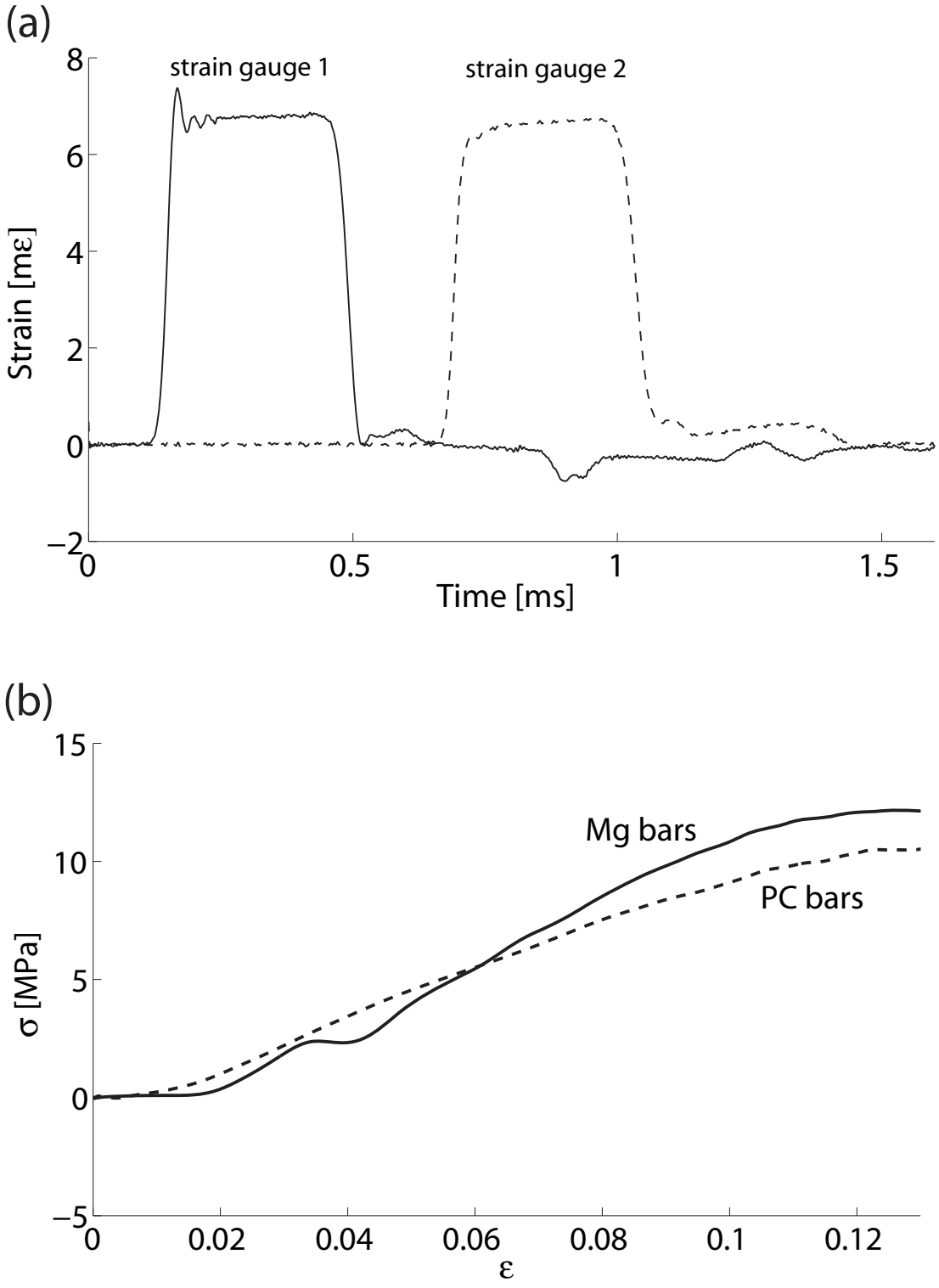

Figure 2: (a) Typical strain response of the long polycarbonate bar measured at two locations along the bar. The impact velocity of the striker is approximately v = 10 m s^{-1}. The distance between the first strain gauge and the second strain gauge is 1.3 m. (b) Compression of Divinycell PVC HD250 foam. Results obtained with polycarbonate pressure bars are compared to results collected using magnesium pressure bars. The tests were conducted at a strain rate of 1500 s^{-1}.

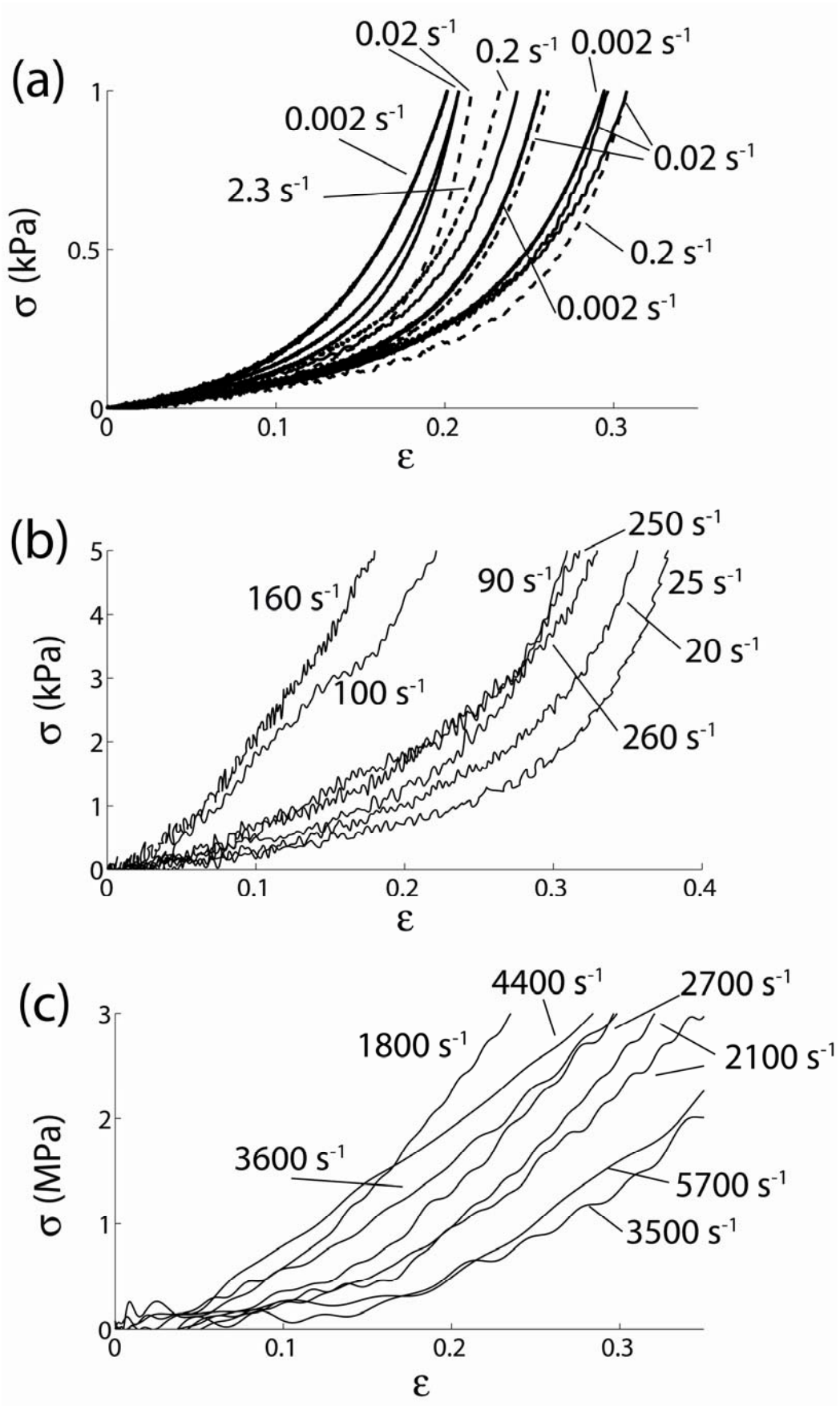

Figure 3: Uniaxial compression of adipose tissue at strain rates (a) $\dot{\varepsilon} = 0.002\ s^{-1} - 0.25\ s^{-1}$. (b) $\dot{\varepsilon} = 20\ s^{-1} - 260\ s^{-1}$. (c) $\dot{\varepsilon} = 1000\ s^{-1}$ - $5700\ s^{-1}$. Data in graph (a) represented by a solid line was measured at 25 ºC, representative data at 37 ºC is shown by a dashed line.

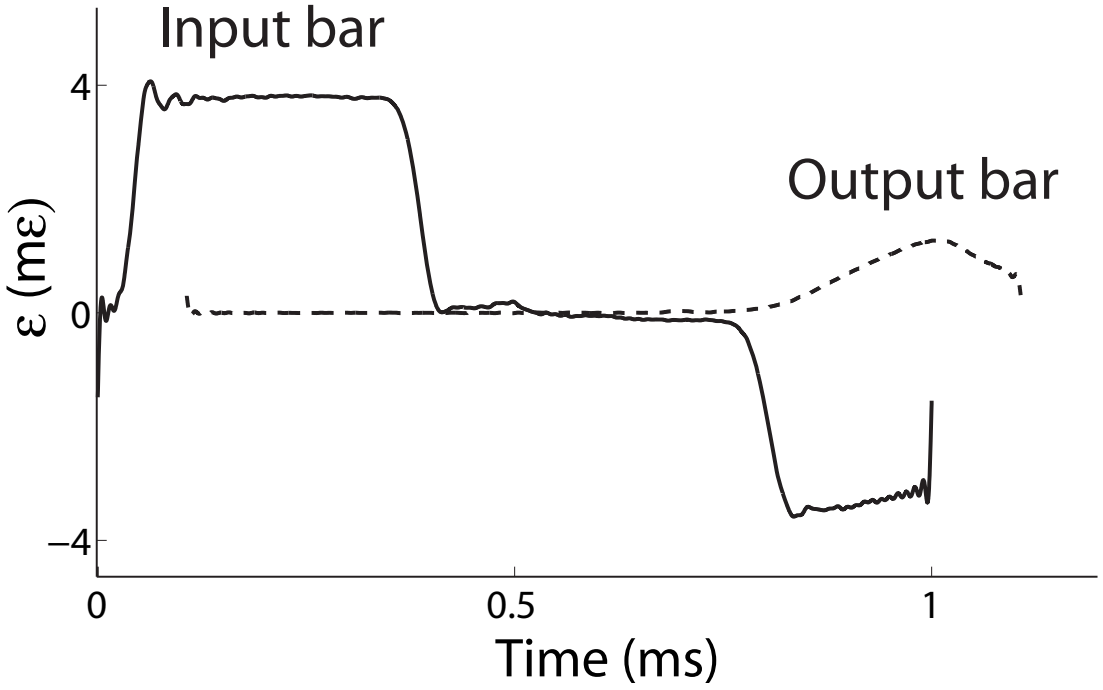

Figure 4: Oscilloscope trace of the compression of adipose tissue using a split Hopkinson pressure bar at a strain-rate of 1840 s^{-1}.

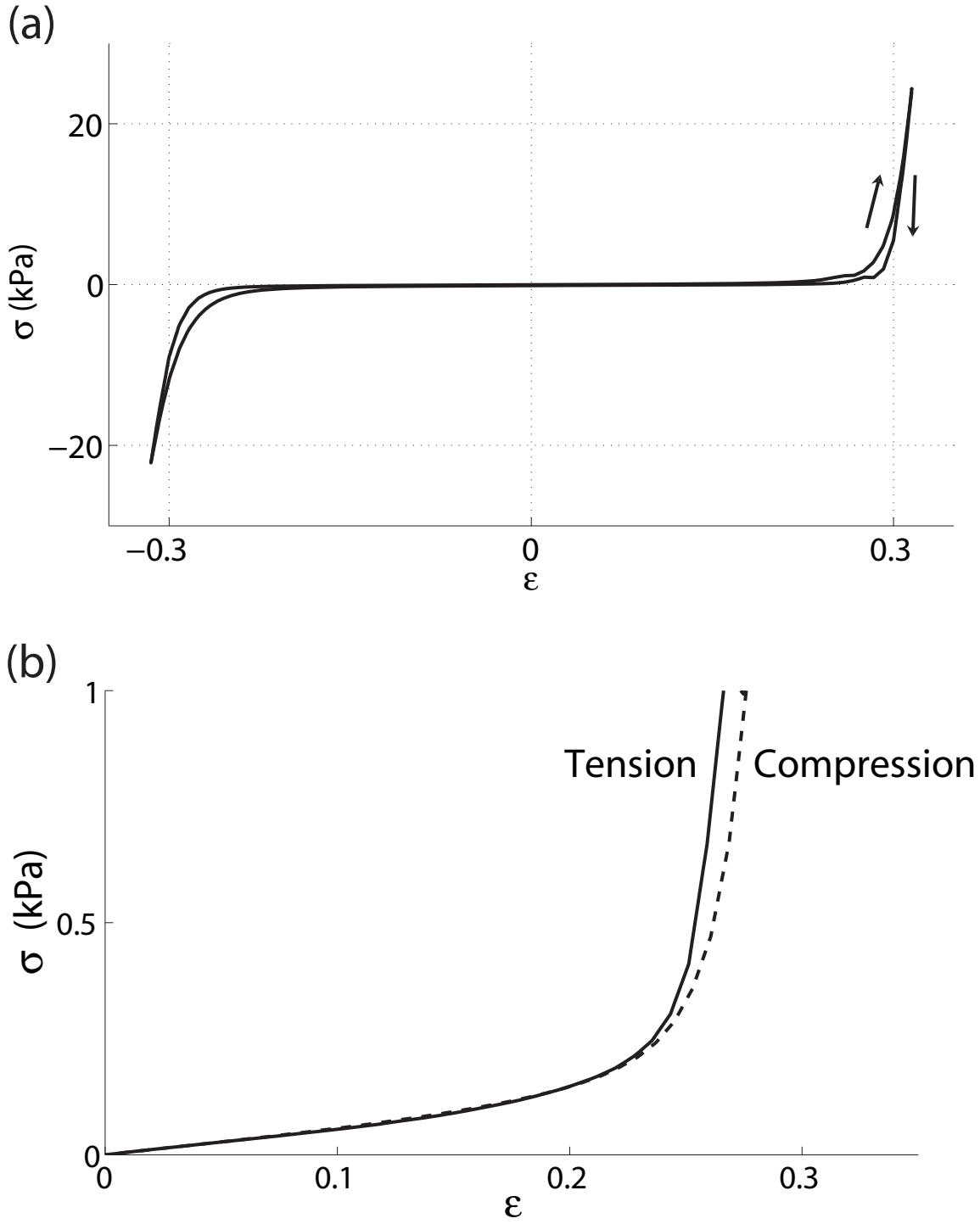

Figure 5: (a) Quasi-static uniaxial compression and tension of adipose tissue averaged over 4 cycles. Arrows show the direction of displacement. The data has been shifted relative to the strain axis so that strain is equi-distant between ± 1 kPa stress. (b) Quasi-static uniaxial tension versus compression of adipose tissue.

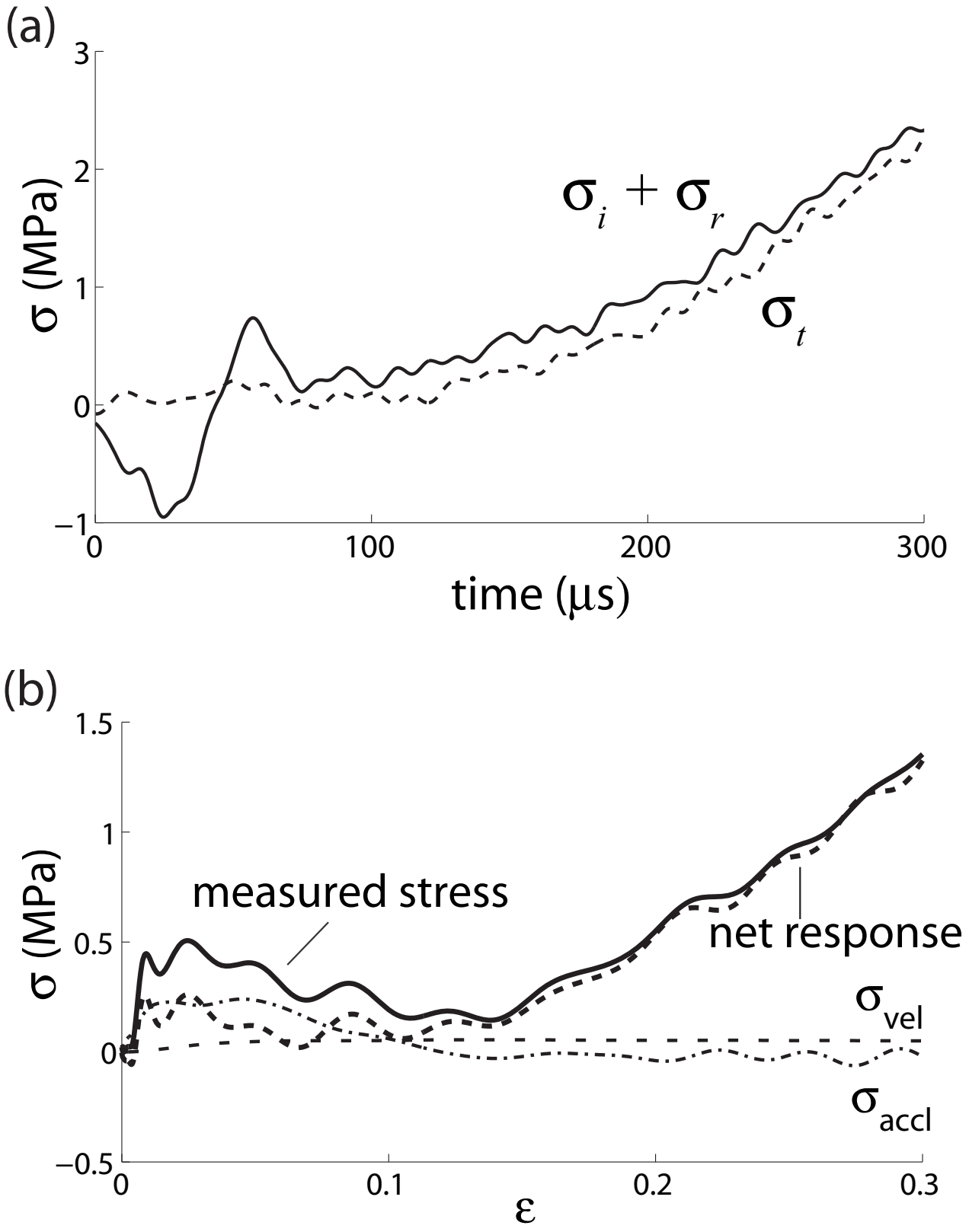

Figure 6: (a) Comparison of input ($\sigma_i + \sigma_r$) and output (σ_t) stress measured by the SHPB to assess the time to reach axial equilibrium. Measurements were taken at a nominal strain rate of 2000 s^{-1}. (b) Comparison of the measured stress with the inertial stresses σ_{vel} and σ_{accel}, described by Eq. (9). The net response is the measured stress less the inertial stresses. The test was conducted at 3500 s^{-1}.

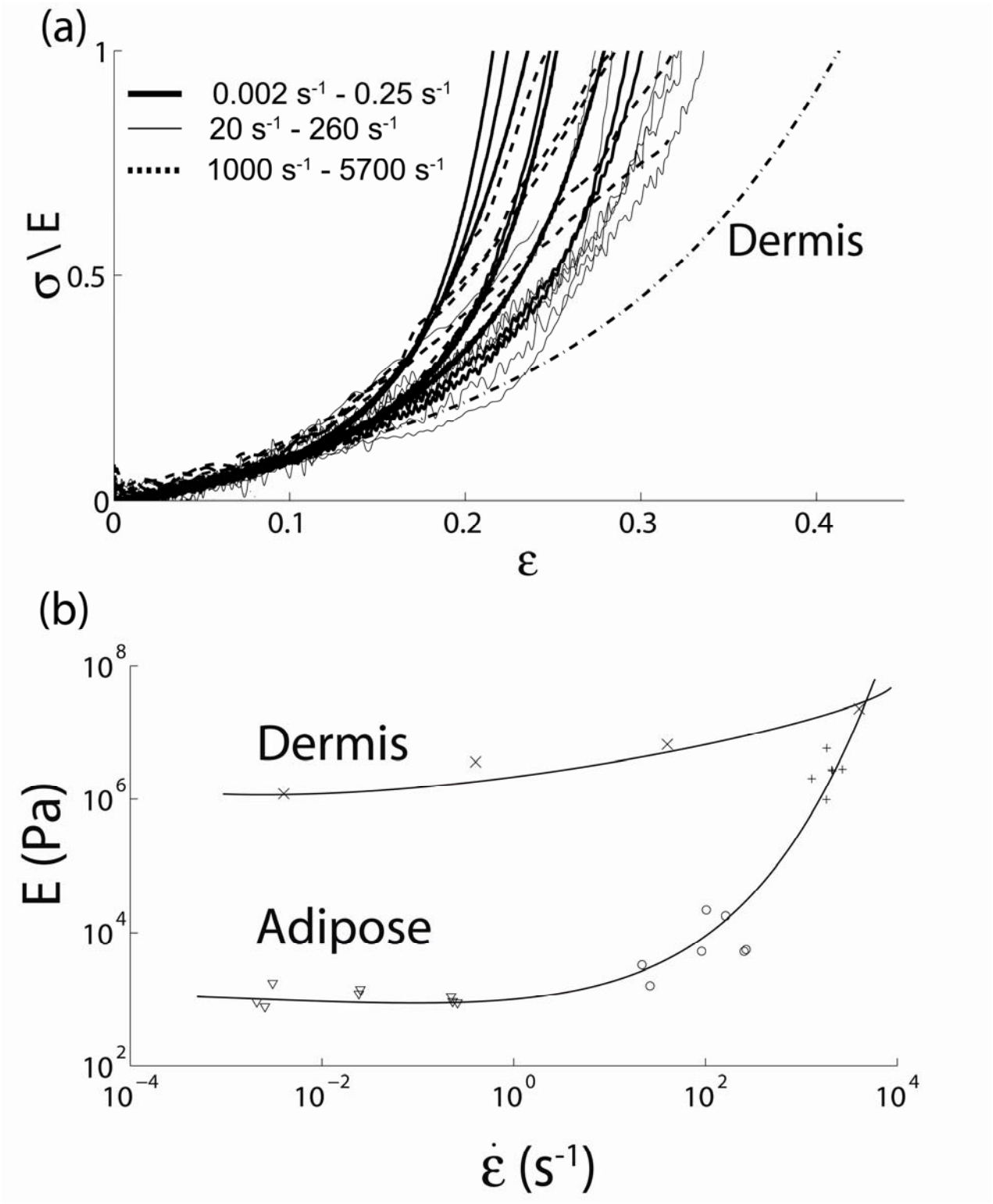

Figure 7: (a) Stress versus strain curves of adipose tissue, normalised by modulus E. The average dermal response measured by Shergold et al. [14] is shown for comparison. (b) Modulus, E (Pa) of adipose tissue under uniaxial compression versus strain rate (s^{-1}). Data shown by triangular markers were measured using a screw-driven tensile test machine, circular markers by a hydraulic test machine and the crosses represent data collected using the SHPB. Diagonal crosses represent the modulus of dermis recorded by Shergold et al. [14].